Journal of Sound and Vibration (2002) **255**(4), 777–788
doi:10.1006/jsvi.2001.4171, available online at http://www.idealibrary.com on IDEAL®

LETTERS TO THE EDITOR

INFLUENCE OF SOME THIN SHELL THEORIES ON THE EVALUATION OF THE NOISE LEVEL IN STIFFENED CYLINDERS

R. RUOTOLO

Department of Aeronautical and Space Engineering, Politecnico di Torino, corso Duca degli Abruzzi 24, *Torino, Italy. E-mail: ruotolo@athena.polito.it*

(*Received* 23 *April* 2001, *and in final form* 12 *September* 2001)

1. INTRODUCTION

The reduction of interior noise is becoming more and more important in various engineering fields. In particular, studies performed by the European Community, and directed to the overall improvement of the cabin environmental conditions for both the passengers and the crew, states that during the next years it will be necessary to reduce cabin noise by 5–10 dB for jets and by 10–15 dB for both turbopropellers and rotorcraft. Furthermore, the problem of reducing interior noise levels is of primary importance for launch vehicles, where sound and structurally induced vibration can damage the payload (indeed, according to reference [1], the vibroacoustic launch environment has been blamed for between 30 and 60% of first day satellite failures), and also for manned space modules, where stringent requirements related to acceptable interior noise levels must be satisfied [2]. As a consequence, tools permitting an accurate prediction of the interior noise level are required.

The prediction of the noise in acoustic cavities is usually performed by developing a mathematical model for both the external structure and the internal cavity. These two models must be coupled, making it possible to determine the effect in the acoustic cavity of a pressure striking the external structure; this is the case of, e.g., an aircraft fuselage or of a launch vehicle. It follows that modifications in the dynamic behaviour of the model of the external structure (e.g., due to the use of different theories) may induce variations in the predicted interior noise. The evaluation of these changes, when the structure is represented by a stiffened cylinder, is addressed in this letter.

Several aerospace structures can be considered as stiffened cylinders, a class of thin shell structures analyzed by a number of researchers; a review of the available literature dealing with their dynamic behaviour can be found in reference [3]. Recently, in a companion paper [4] natural frequencies of stiffened cylinders have been evaluated according to the thin shell theories of Donnell, Sanders, Love and Flügge, and it has been demonstrated that, in some cases, Donnell's theory leads to very high errors in the evaluation of eigenfrequencies of such structures.

Several authors addressed the problem of predicting interior noise levels into the fuselage of propeller-driven aircraft. In several previous works, different thin shell theories were used to determine the vibroacoustic behaviour of stiffened cylinders (e.g., in references [5–8] Donnell's theory was used, in references [9–11] Flügge's theory, while in reference [12] Cole III used Love–Timoshenko's theory).

Nevertheless, despite the great research activity spent in analyzing the dynamic response of stiffened cylinders, as demonstrated in reference [3], and to predict the cabin noise in

0022-460X/02/$35.00

propeller-driven aircraft, to the best of the author's knowledge no investigations have been performed to determine the influence of inaccuracies of the thin shell model on the interior noise level prediction of stiffened cylinders.

In this letter, a family of stiffened cylinders subjected to random excitation and with a different ring dimension is analyzed with the aim of determining the influence of the structural theory on the interior noise. Finally, some numerical simulations are presented regarding the noise field due to harmonic and random excitations in an aircraft fuselage without the floor and similar to those analyzed in references [8, 13–15].

2. EVALUATION OF THE INTERIOR NOISE LEVEL

In the following, a cylinder with length L and radius R is considered. The cylinder is assumed to be simply supported at both ends, a boundary condition which is satisfied by the following functions for axial, circumferential and radial displacements respectively:

$$u^0(x,\theta) = \sum_{m,n} [U_{s;m,n}\phi^{(U)}_{s;m,n}(x,\theta) + U_{a;m,n}\phi^{(U)}_{a;m,n}(x,\theta)],$$

$$v^0(x,\theta) = \sum_{m,n} [V_{s;m,n}\phi^{(V)}_{s;m,n}(x,\theta) + V_{a;m,n}\phi^{(V)}_{a;m,n}(x,\theta)],$$

$$w(x,\theta) = \sum_{m,n} [W_{s;m,n}\phi^{(W)}_{s;m,n}(x,\theta) + W_{a;m,n}\phi^{(W)}_{a;m,n}(x,\theta)], \tag{1}$$

where

$$\phi^{(U)}_{s;m,n}(x,\theta) = \cos(m\pi x/L)\cos(n\theta),$$

$$\phi^{(V)}_{s;m,n}(x,\theta) = \sin(m\pi x/L)\sin(n\theta),$$

$$\phi^{(W)}_{s;m,n}(x,\theta) = \sin(m\pi x/L)\cos(n\theta) \tag{2}$$

for symmetrical displacements and

$$\phi^{(U)}_{a;m,n}(x,\theta) = \cos(m\pi x/L)\sin(n\theta),$$

$$\phi^{(V)}_{a;m,n}(x,\theta) = \sin(m\pi x/L)\cos(n\theta),$$

$$\phi^{(W)}_{a;m,n}(x,\theta) = \sin(m\pi x/L)\sin(n\theta) \tag{3}$$

for antisymmetrical displacements. The stiffness matrix $[\mathbf{K}_{m,n}]$ is given in Appendix B of reference [4]. Moreover, the mass matrix $[\mathbf{M}_{m,n}]$ is evaluated according to the averaging approach.

Given a distributed external pressure $p_e(x,\theta,\omega)$ acting on the surface of the fuselage, the motion of the sidewall is determined by taking advantage of the orthogonality of functions (2) and (3) when integrated over the surface of the cylinder. As a consequence, coefficients $U_{m,n}$, $V_{m,n}$ and $W_{m,n}$ are given by

$$[U_{\alpha;m,n}\ \ V_{\alpha;m,n}\ \ W_{\alpha;m,n}]^{\mathrm{T}} = ((1+\mathrm{j}\eta_s)[\mathbf{K}_{\alpha;m,n}] - \omega^2[\mathbf{M}_{m,n}])^{-1}\ \lfloor\ 0\ \ 0\ f_{\alpha;m,n}\ \rfloor^{\mathrm{T}}, \tag{4}$$

with $\alpha = s, a$ for symmetrical and antisymmetrical motion, respectively, η_s the structural damping, ω the circular frequency of the excitation; modal forces are given by

$$f_{\alpha;m,n}(\omega) = \int_0^{2\pi} \int_0^L p_e(x, \theta, \omega)\, \phi^{(W)}_{\alpha;m,n}(x, \theta)\, \mathrm{d}x\, R\, \mathrm{d}\theta. \tag{5}$$

The mathematical model of the acoustic cavity in the cylinder is determined by following the same procedure described in references [13–15]. Natural circular frequencies of the cavity are given by [16]

$$\omega^A_{n_1,n_2,n_3} = c\sqrt{\left(\frac{n_1\pi}{L}\right)^2 + k^2_{n_2,n_3}}, \tag{6}$$

where Rk_{n_2,n_3} is the n_3rd root of $\mathrm{J}'_{n_2}(s)$, $\mathrm{J}_{n_2}(s)$ being the Bessel function of first kind and order n_2. Symmetrical mode shapes are

$$F_{s;n_1,n_2,n_3}(x, r, \theta) = \cos(n_1\pi x/L)\cos(n_2\theta)\mathrm{J}_{n_2}(k_{n_2,n_3} r) \tag{7}$$

and the antisymmetrical are

$$F_{a;n_1,n_2,n_3}(x, r, \theta) = \cos(n_1\pi x/L)\sin(n_2\theta)\mathrm{J}_{n_2}(k_{n_2,n_3} r). \tag{8}$$

The structural acoustic coupled problem is solved assuming that the effects of the internal pressure on the displacements of the cylinder sidewall are negligible, so that the interior noise level can be predicted by applying the method proposed by Dowell *et al.* [17].

Since the sidewalls of the cylinder are flexible, the pressure level of the internal cavity can be predicted by solving the wave equation with the following boundary conditions on the sidewalls:

$$\left.\frac{\partial p}{\partial \mathbf{n}}\right|_{r=R} = -\rho_a \ddot{w}(x, \theta), \qquad \left.\frac{\partial p}{\partial x}\right|_{x=0,\, x=L} = 0, \tag{9}$$

where $\mathbf{n}$ and $w(x, \theta)$ are the normal to and the out-of-plane displacement of the cylinder sidewall, respectively; moreover ρ_a is the air density.

The internal pressure can be written by applying modal superposition of symmetrical and antisymmetrical modes

$$p(x, r, \theta, \omega) = \sum_{n_1,n_2,n_3} \left[\frac{P_{s;n_1,n_2,n_3}(\omega)\, F_{s;n_1,n_2,n_3}(x, r, \theta)}{M_{s;n_1,n_2,n_3}} + \frac{P_{a;n_1,n_2,n_3}(\omega)\, F_{a;n_1,n_2,n_3}(x, r, \theta)}{M_{a;n_1,n_2,n_3}}\right], \tag{10}$$

where M_{n_1,n_2,n_3} is the modal mass of the (n_1, n_2, n_3) mode of the acoustic cavity

$$M_{n_1,n_2,n_3} = \frac{1}{V}\int_0^{2\pi}\int_0^R\int_0^L F_{n_1,n_2,n_3}(x, r, \theta)^2 r\, \mathrm{d}\theta\, \mathrm{d}r\, \mathrm{d}x \tag{11}$$

evaluated for both symmetric and antisymmetric modes as shown in reference [18] and with the volume of the acoustic cavity given by $V = \pi R^2 L$.

The out-of-plane motion of the cylinder sidewall can be written according to equation (1) by using modal superposition, so that it follows [17]

$$P_{s;n_1,n_2,n_3}(\omega) = \frac{\rho_a c^2 \omega^2 A_f}{V} \frac{\sum_{m,n} W_{s;m,n}(\omega) L_{s;n_1,n_2,n_3,m,n}}{(1 + j\eta_a)(\omega^A_{n_1,n_2,n_3})^2 - \omega^2}, \tag{12}$$

where A_f is the surface of the cylinder sidewall, $2\pi RL$, and $L_{s;n_1,n_2,n_3,m,n}$ is the interaction factor between the (n_1, n_2, n_3) acoustic and the (m, n) structural mode

$$L_{s;n_1,n_2,n_3,m,n} = \frac{1}{A_f} \int_0^{2\pi} \int_0^L F_{s;n_1,n_2,n_3}(x, R, \theta) \phi^{(W)}_{s;m,n}(x, \theta) R \, d\theta \, dx \tag{13}$$

and its expression is given in reference [18]. The modal pressure for antisymmetrical modes is calculated similarly.

The internal pressure at every point of the acoustic cavity is determined by introducing equation (12) into equation (10)

$$\begin{aligned} p(x, r, \theta, \omega) = & \sum_{n_1,n_2,n_3} \frac{\rho_a c^2 \omega^2 A_f}{V((1 + j\eta_a)(\omega^A_{n_1,n_2,n_3})^2 - \omega^2)} \\ & \times \left(\sum_{m,n} W_{s;m,n}(\omega) L_{s;n_1,n_2,n_3,m,n} F_{s;n_1,n_2,n_3}(x, r, \theta)/M_{s;n_1,n_2,n_3} \right. \\ & \left. + \sum_{m,n} W_{a;m,n}(\omega) L_{a;n_1,n_2,n_3,m,n} F_{a;n_1,n_2,n_3}(x, r, \theta)/M_{a;n_1,n_2,n_3} \right). \end{aligned} \tag{14}$$

3. NUMERICAL EXAMPLES

3.1. PARAMETRIC ANALYSIS

In this section, results of a parametric investigation regarding three stiffened cylinders subjected to random excitation are shown.

Every cylinder has the same properties of the simple fuselage model analyzed in the next section (see Table 1) with the exception of the wall thickness h that is equal to 3 mm, and of the geometrical properties of the stiffeners, listed in Table 2. According to this table, the value of the γ_D factor† for these three cylinders (cases A–C) is 14·25, 164·11 and 921·56 respectively. As a consequence, errors in the prediction of natural frequencies related to Donnell's theory increase through cases A–C.

The simulation has been performed by exciting the cylinder with two full correlated random forces located at the points $(x = L/2, \theta = 90^\circ)$ and $(x = L/2, \theta = 270^\circ)$ and with equal magnitude. As a consequence, the external pressure distribution can be written as

$$p_e(x, \theta, \omega) = (\delta(x - L/2)\delta(\theta - 90^\circ) + \delta(x - L/2)\delta(\theta - 270^\circ)) p_t(\omega), \tag{15}$$

where $p_t(\omega)$ has a constant power spectral density (PSD) equal of 1 Pa^2/Hz over the frequency range from 10 to 400 Hz.

†This factor was introduced in reference [4] and is an index of the accuracy of results provided by Donnell's theory: for $\gamma_D \gg 1$ results are very poor.

TABLE 1

Properties of both a simple aircraft fuselage and of its acoustic cavity

d	Constant for propeller pressure	2
k_1	Constant for propeller pressure (at $1 \times$ BPF)	1·5
k_2	Constant for propeller pressure (at $2 \times$ BPF)	3
x_0	Propeller plane	3·5 (m)
θ_0	Angles for propeller pressure	85° (deg)
θ_1	Angles for propeller pressure	0° (deg)
θ_2	Angles for propeller pressure	150° (deg)
P_1	Propeller peak pressure (at $1 \times$ BPF)	150 (N/m^2)
P_2	Propeller peak pressure (at $2 \times$ BPF)	111·7 (N/m^2)
ω	Propeller BPF	88 (Hz)
h	Wall thickness	1·2 (mm)
R	Fuselage radius	1·3 (m)
L	Fuselage length	16 (m)
η_s	Structural damping	0·01
η_a	Acoustic damping	0·01
c_0	Speed of sound	343 (m/s)
ρ_a	Air density	1·21 (kg/m^3)
E	Young's modulus	$7{\cdot}1 \times 10^{10}$ (N/m^2)
ρ	Material density	2700 (kg/m^3)
v	Poisson's ratio	0·31
A_s	Stringer area	$4{\cdot}88 \times 10^{-5}$ (m^2)
d_s	Distance between two stringers	0·40 (m)
z_s	Stringer centre of mass	−0·00734 (m)
I_s	Stringer moment of inertia	$1{\cdot}577 \times 10^{-9}$ (m^4)
A_r	Ring area	$2{\cdot}57 \times 10^{-4}$ (m^2)
d_r	Distance between two rings	0·40 (m)
z_r	Ring centre of mass	− 0·045 (m)
I_r	Ring moment of inertia	$2{\cdot}966 \times 10^{-7}$ (m^4)

TABLE 2

Geometrical properties of stringers and rings for the family of stiffened cylinders used in the parametric analysis

		Case A	Case B	Case C
Stringers	$A_s \times 10^6$ (m^2)	69·12	69·12	69·12
	$I_s \times 10^9$ (m^4)	4·792	4·792	4·792
	d_s (m)	0·4	0·4	0·4
	z_s (mm)	−11·5	−11·5	−11·5
Rings	$A_r \times 10^6$ (m^2)	69·12	117·1	189·1
	$I_r \times 10^9$ (m^4)	4·792	60·61	332·0
	d_r (m)	0·4	0·4	0·4
	z_r (mm)	−11·5	−31·5	−61·5
	γ_D	14·25	164·11	921·56

The PSD of the internal pressure level was evaluated by calculating firstly the frequency response function between the two excitation points and the considered response location inside the cylinder. Power spectral densities for the three cases are shown in Figures 1–3 where continuous and dash–dot lines are related to Flügge's and Donnell's results respectively.

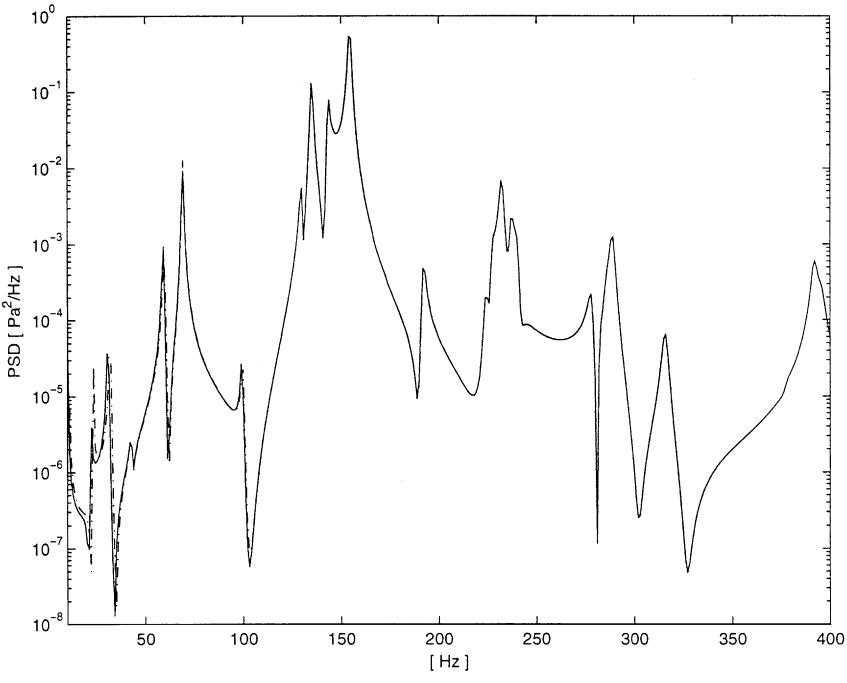

Figure 1. Comparison of internal pressure PSD for case A (——, Flügge's; – · –, Donnell's theory).

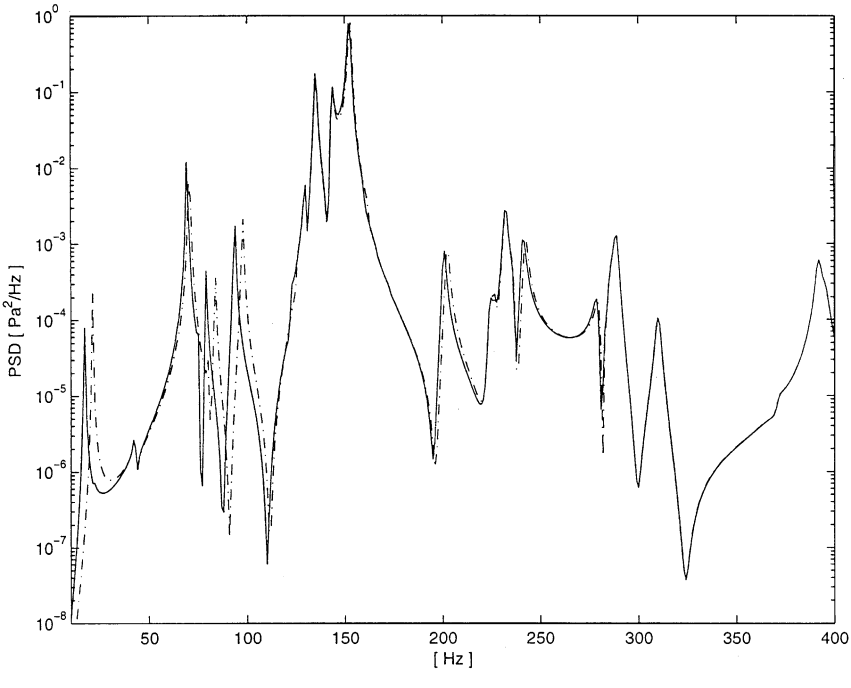

Figure 2. Comparison of internal pressure PSD for case B (——, Flügge's; – · –, Donnell's theory).

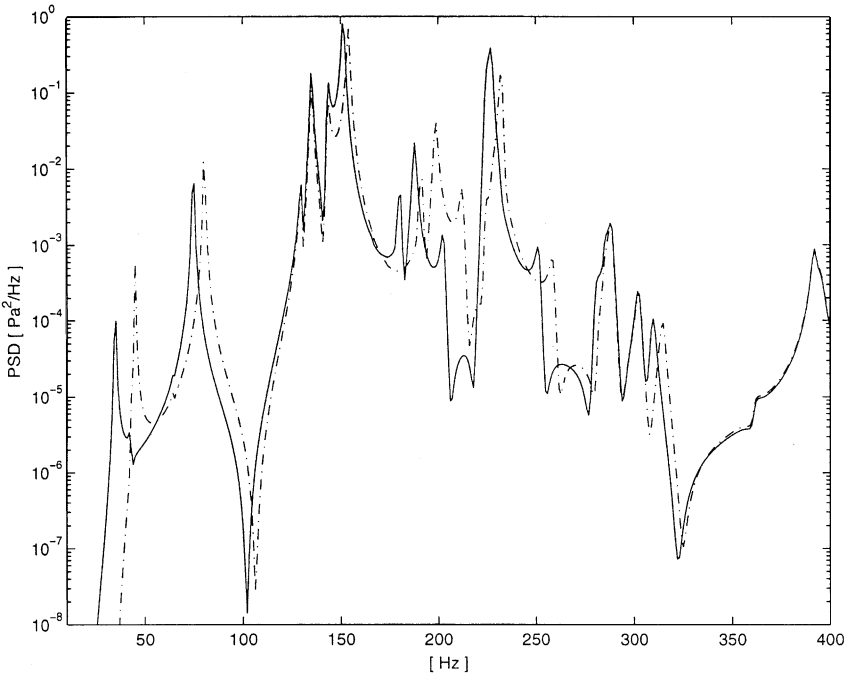

Figure 3. Comparison of internal pressure PSD for case C (——, Flügge's; – · –, Donnell's theory).

By comparing these three figures, it appears that errors in the prediction of the dynamic properties of a stiffened cylinders affect mainly the internal pressure PSD at low frequencies. By increasing the dimension of the stiffeners, so that both γ_D and errors in eigenfrequencies increase, the frequency range with errors in the PSD expands at higher frequencies. Moreover, these figures demonstrate that for structures having γ_D up to 10–20, differences of interior noise levels due to the use of a different thin shell theory can be neglected.

In Figure 4(a) and 4(b) the ratio between the PSD evaluated by using Sanders' and Love's theories, respectively, to the PSD calculated through Flügge's theory is illustrated. Since this result is related to case C, i.e., that with the largest rings, it follows that discrepancies in the results obtained by using these three theories to determine the interior noise for the cases A and B are smaller. Figure 4(a) and 4(b) demonstrates that the use of Sanders', Love's and Flügge's theory for the shell gives very close results in terms of interior noise: a maximum relative difference of 0·4% between corresponding PSDs has been obtained.

3.2. AIRCRAFT FUSELAGE

In this section is considered a simple fuselage structure without the floor, already used in a numerical example in reference [4] and with $\gamma_D = 8592$; properties of the entire model, i.e., of both the structure and the internal cavity, and listed in Table 1. Two comparisons are shown, one related to harmonic and the other to random excitation, aimed to illustrate the influence on the prediction of internal pressure of different thin shell theories.

3.2.1. *Harmonic excitation*

In this example, it is assumed that the fuselage is exerted by the external pressure due to the presence of one propeller. By using experimental data, Thomas *et al.* [13] determined

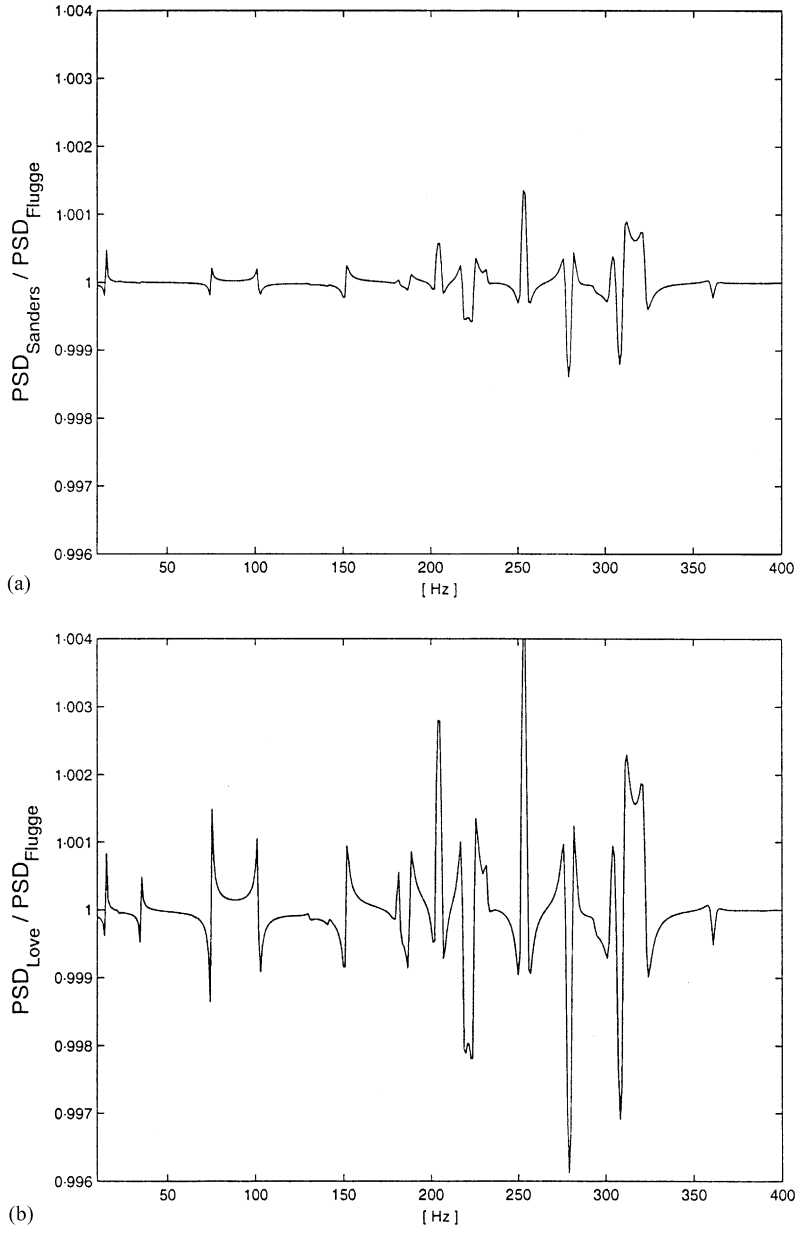

Figure 4. Ratio between internal pressure PSD obtained by using Sanders' (a) and Love's (b) theory and Flügge's theory.

the following expression for the pressure distribution of the propeller of a British Aerospace aircraft with 48 passengers:

$$p_e(x, \theta) = p_{e;x}(x)\, p_{e;\theta}(\theta) \tag{16}$$

with

$$p_{e;x}(x) = \begin{cases} e^{-d(x_0 - x)}, & x \in [0, x_0], \\ e^{-d(x - x_0)}, & x \in [x_0, L], \end{cases}$$

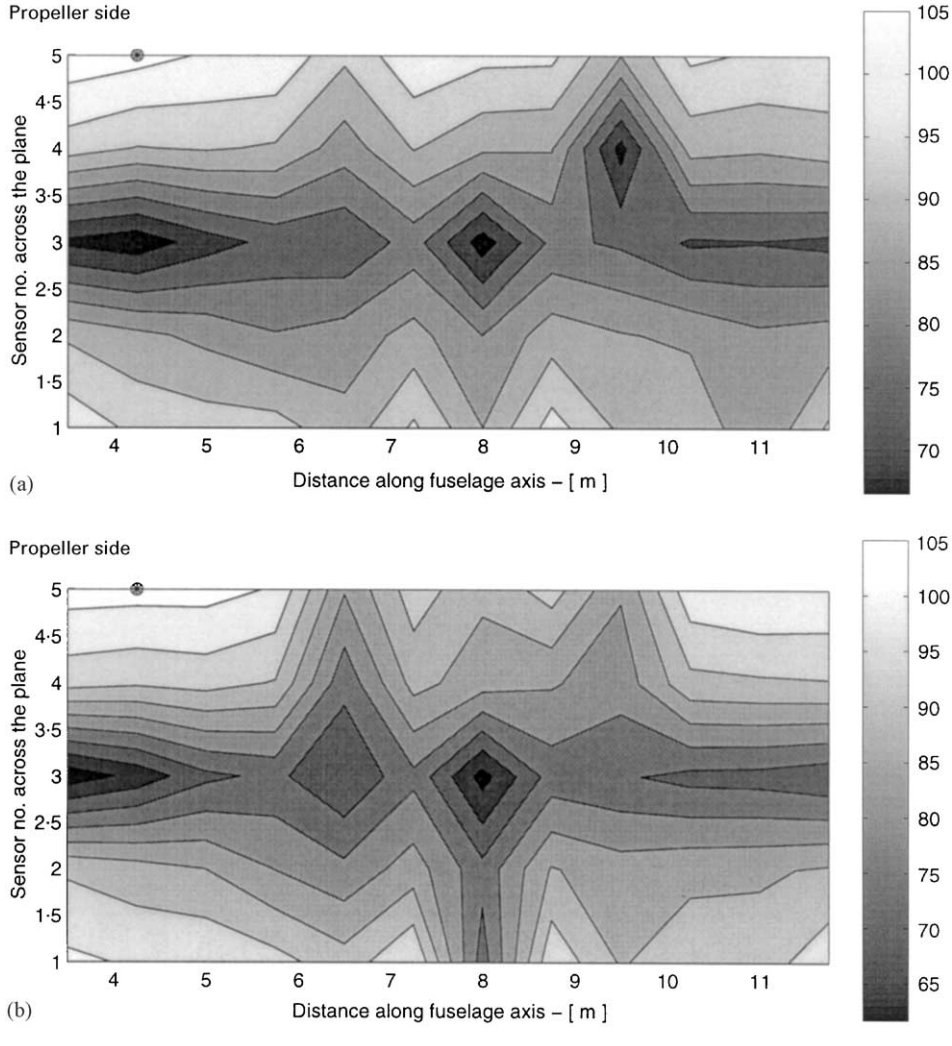

Figure 5. Internal pressure on the head plane for harmonic excitation at a frequency of 176 Hz, (a) Donnell's and (b) Flügge's theory.

$$p_{e;\theta}(\theta) = \begin{cases} \dfrac{\theta - \theta_1}{\theta_0 - \theta_1} e^{jk_\theta(\theta_0 - \theta)}, & \theta \in [\theta_1, \theta_0], \\ \dfrac{\theta_2 - \theta}{\theta_2 - \theta_0} e^{jk_\theta(\theta_0 - \theta)}, & \theta \in [\theta_0, \theta_2], \end{cases} \tag{17}$$

where d and k_θ are determined by properly analyzing the experimental data and represent reduction factors of the pressure distribution with respect to the pressure at (x_0, θ_0) that is the nearest point of the fuselage to the propeller disk. Moreover, θ_1 and θ_2 indicate the extent of the pressure distribution over the fuselage.

The noise level into the fuselage at the passengers' head plane has been evaluated according to the procedure described in Section 2 and results at $2 \times$ BPF are shown in Figure 5. It appears that the maximum predicted pressure levels are in close agreement between the two theories even if the pressure distribution over the passengers' head plane is

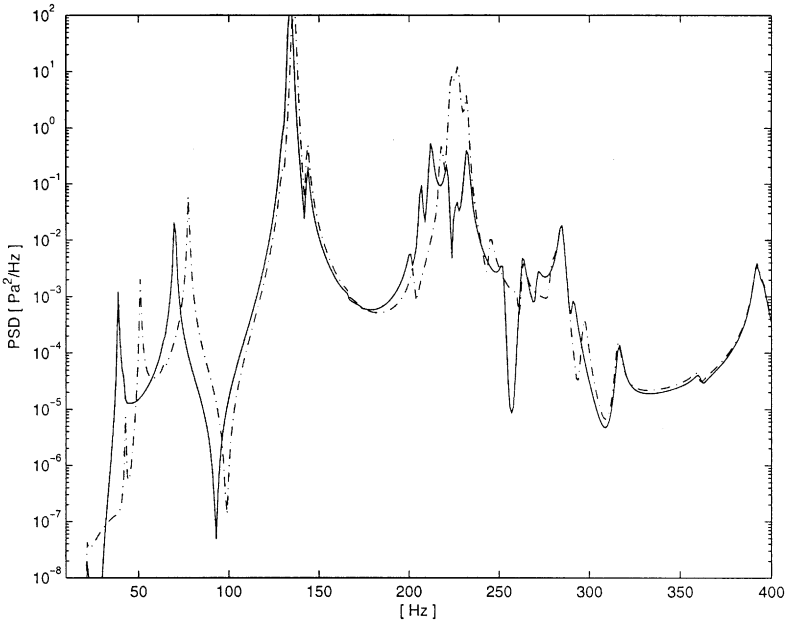

Figure 6. Comparison of internal pressure PSD on the passengers' head plane (——, Flügge's; – · –, Donnell's theory).

different. This is an indication that structural and acoustic interacting modes may change by using different thin shell theories. Finally, the two levels of overall noise for an excitation at both $1 \times$ BPF and $2 \times$ BPF are very similar: 104·4 and 104·1 dB for Donnell and Flügge's theory respectively.

3.2.2. *Random excitation*

In this example, the same random excitation described in Section 3.1 for the parametric analysis has been used.

The PSD of the internal pressure for a point located near the propeller plane and over the passengers' head plane (shown by the circle in Figure 5) is illustrated in Figure 6, where continuous and dash–dot lines are related to Flügge's and Donnell's results respectively. These figures show that the shift of natural frequencies predicted by using the two thin shell theories may give rise to a corresponding shift of the trend of the response (this is particularly evident in the frequency range from 50 to 100 Hz). Moreover, the magnitude of the response may be different. Figure 7 illustrates the effect on the predicted sound pressure level, evaluated over a 1/3 octave band, of the use of the two structural theories: it is clear from this figure that the maximum difference in the response is in the low-frequency range.

4. CONCLUSIONS

In this letter Love's, Donnell's, Flügge's and Sanders' thin shell theories are used to evaluate the internal pressure in both a family of stiffened cylinders with rings of different dimensions and in the model of a fuselage without the floor subjected to harmonic and random excitations.

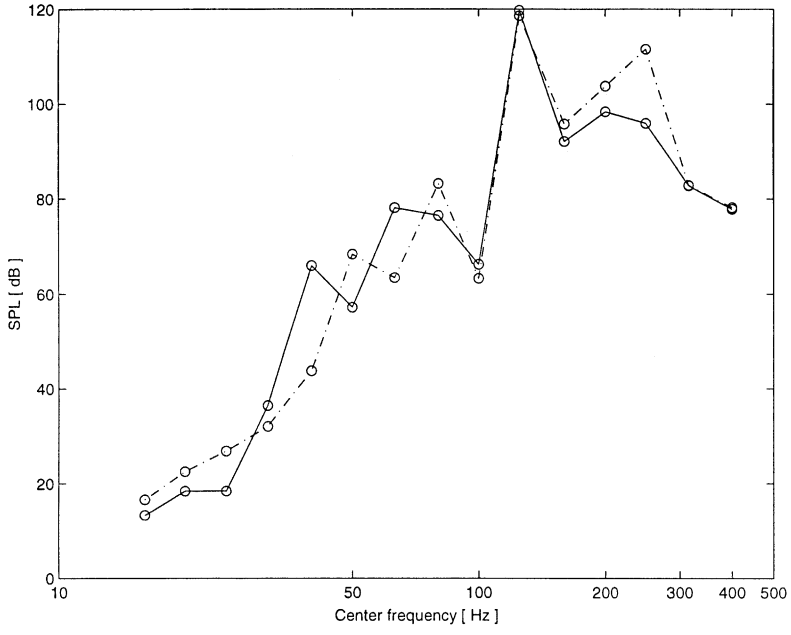

Figure 7. Comparison of sound pressure level (1/3 octave band) on the passengers' head plane (——, Flügge's; – · –, Donnell's theory).

It is demonstrated that Donnell's theory may provide different results from those obtained by applying the other three thin shell theories in terms of pressure distribution over the passengers' head plane and low-frequency spectrum of the internal pressure even if, for the considered harmonic excitation, the overall and maximum noise levels are less than 1 dB higher than those predicted by using the other theories for the shell structure. Differences in the predicted interior noise are due to eigenfrequencies errors related to the use of Donnell's theory, so that by using only material and geometrical properties of the structure, the ratio γ_D [4] can be used to establish *a priori* if Donnell's theory can or cannot provide good results.

REFERENCES

1. A. TIMMINS and R. HEUSER 1971 *NASA* TND-6474. A study of first day malfunctions.
2. NASA-STD-3000, 1991. *Space Station Man Systems Integration*, Vol. 4, Rev. A.
3. M. MUKHOPADHYAY and G. SINHA 1992 *Shock and Vibration Digest* **24**, 3–13. A review of dynamic behaviour of stiffened shells.
4. R. RUOTOLO 2001 *Journal of Sound and Vibration* **243**, 847–860. A comparison of some thin shell theories for the dynamic analysis of stiffened cylinders.
5. L. D. POPE, D. C. RENNISON, C. M. WILLIS and W. H. MAYES 1982 *Journal of Sound and Vibration* **82**, 541–575. Development and validation of preliminary analytical models for aircraft interior noise prediction.
6. L. D. POPE, E. G. WILBY, C. M. WILLIS and W. H. MAYES 1983 *Journal of Sound and Vibration* **89**, 371–417. Aircraft interior noise models: sidewall trim, stiffened structures and cabin acoustics with floor partition.
7. J. E. COLE III, A. W. STOKES, J. M. GARRELICK and K. F. MARTINI 1988 *NASA CR* 4136. Analytical modeling of the structureborne noise path on a small twin-engine aircraft.
8. C. R. FULLER, J. P. MAILLARD, M. MERCADAL and A. H. VON FLOTOW 1997 *Journal of Sound and Vibration* **203**, 754–761. Control of aircraft interior noise using globally detuned vibration absorbers.

9. M. PETYT and J. WEI 1997 *Proceedings of the Japan International Modal Analysis Conference, Tokyo*, 647–653. Free vibration of an idealized fuselage structure.
10. M. PETYT and J. WEI 1998 *Proceedings 23rd International Seminar on Modal Analysis, Leuven*, 699–706. Prediction of propeller-induced interior sound fields in aircraft.
11. L. R. KOVAL 1980 *Journal of Sound and Vibration* **71**, 511–521. On sound transmission into a stiffened cylindrical shell with rings and stringers treated as discrete elements.
12. J. E. COLE III 1997 *Computers and Structures* **65**, 385–393. Vibrations of a framed cylindrical shell submerged in and filled with acoustic fluids: spectral solution.
13. D. R. THOMAS, P. A. NELSON and S. J. ELLIOTT 1993 *Journal of Sound and Vibration* **167**, 91–111. Active control of the transmission of sound through a thin cylindrical shell. Part I: the minimization of vibrational energy.
14. D. R. THOMAS, P. A. NELSON and S. J. ELLIOTT 1993 *Journal of Sound and Vibration* **167**, 113–128. Active control of the transmission of sound through a thin cylindrical shell. Part II: the minimization of acoustic potential energy.
15. A. J. BULLMORE, P. A. NELSON and S. J. ELLIOTT 1990 *Journal of Sound and Vibration* **140**, 191–217. Theoretical studies of the active control of propeller-induced cabin noise.
16. F. FAHY 1987 *Sound and Structural Vibration — Radiation, Transmission and Response*. London: Academic Press Ltd.
17. E. H. DOWELL, G. F. GORMAN III and D. A. SMITH 1977 *Journal of Sound and Vibration* **52**, 519–542. Acoustoelasticity: general theory, acoustic natural modes and forced response to sinusoidal excitation, including comparisons with experiments.
18. R. RUOTOLO 1998 *Technical Report no.* 137, *Department of Aeronautical and Space Engineering, Politecnico di Torino*. Evaluation of internal noise for a propeller driven aircraft (in Italian).